Peer-reviewed version available at Int. J. Mol. Sci. 2018, 19, 3488; doi:10.3390/ijms19113488

Article

Metformin Hydrochloride-Plga Nanoparticles in Diabetic Rats in A Periodontal Disease Experimental Model

Aline de Sousa Barbosa Freitas Pereira [1], Gerly Anne de Castro Brito [2], Maria Laura de Souza Lima [1], Arnóbio Antônio da Silva Júnior [3], Emanuell dos Santos Silva [4], Adriana Augusto de Rezende [4], Raul Hernandes Bortolin [4], Maria Galvan [5], Flávia Q. Pirih [5], Raimundo Fernandes de Araújo Júnior [6], Caroline Addison Carvalho Xavier de Medeiros [7], Gerlane Coelho Bernando Guerra [8] and Aurigena Antunes de Araújo [9,*]

[1] Post-graduation program in Odontology Science, Department of Dentistry, UFRN, Natal, RN, Brazil
[2] Post-graduation program in Pharmacology/Post-graduation program in Morphology, Department of Morphology, UFC, Fortaleza, Ceará, Brazil
[3] Department of Pharmacology, Post-graduation program in Pharmaceutical science/Health Science, UFRN, Natal, RN, Brazil
[4] Department of Pharmacology, Post-graduation program in Pharmaceutical science, UFRN, Natal, RN, Brazil
[5] Periodontics Section, School of Dentistry, University of California, UCLA, Los Angeles, USA
[6] Post-graduation program in Functional and Structural Biology/Post-graduation program Health Science/Department of Morphology, UFRN, Natal, RN, Brazil
[7] Post-graduation program Biological Science/Post-graduation program in RENORBIO, Department of Biophysics and Pharmacology, UFRN, Natal, RN, Brazil
[8] Post-graduation program Biological Science/Post-graduation program in Pharmaceutical Science, Department of Biophysics and Pharmacology, UFRN, Natal, RN, Brazil
[9] Post-graduation program Public Health/Post-graduation program in Pharmaceutical Science, Department of Biophysics and Pharmacology, UFRN, Natal, RN, Brazil
* Correspondence: Aurigena Antunes de Araújo. Departamento de Biofisica e Farmacologia, Av. Senador Salgado Filho, S/N, Campus Universitário, Lagoa Nova, 59072-970, UFRN, Natal, RN, Brasil.E-mail:aurigena@ufrnet.br

Abstract: The aim of this study was synthesize and evaluate the effects of Poly (D, L-Lactide-co-glycolide) (PLGA) Nanoparticles (NPs) of metformin (PLGA+ Met) on inflammation, and bone loss in a ligature-induced periodontitis rat model. The prepared NPs were characterized by mean diameter, size particle, polydispensity index and encapsulation efficiency by Atomic force microscopy (AFM). Male albino Wistar rats were randomly divided into four groups of 20 rats in each group, and given the following treatments for 10 days to evaluate *in vivo* activity: (1) Sham: no ligature + water; (2) Positive control: ligature + water (with Periodontal disease and Diabetes); (3) ligature + PLGA+ 10 mg/kg Met (With Periodontal disease and Diabetes); and (4) ligature + PLGA+ 100 mg/kg Met (with Periodontal disease and Diabetes). Water or PLGA + Met was administered orally by gavage. Maxillae were fixed and scanned using Micro-computed Tomography (μCT) to quantify linear of bone loss. Histopathological characteristics were assessed through immunohistochemical staining for Osteocalcin, Cathepsyn K, RANKL/RANK/OPG pathway. IL-1β and TNF-α from gingival tissues were analysed by Elisa immunoassay. Quantitative RT-PCR reaction was used to evaluate gene expression of *AMPK*, *NF-κB p-65*, *Hmgb1* and *TAK-1* from gingival tissues. Statistical analysis was performed using one-way ANOVA at 5% significance. The mean diameter of MET-loaded PLGA nanoparticles was in a range of 457.1 ± 48.9 nm with a polydispersity index of 0.285, zeta potential: 8.16 ± 1.1 mV and entrapment efficiency (EE) was 70%. The results suggest that the addition of MET in the core slightly affected the particle sizes. Treatment with PLGA+ 10 mg/kg Met showed low inflammatory cells, decreased bone loss and integrity cement and levels of IL-1β, and TNF-α ($p < 0.05$) were significantly reduced. Additionally, weak

Peer-reviewed version available at Int. J. Mol. Sci. 2018, 19, 3488; doi:10.3390/ijms19113488

staining was shown by RANKL, Cathepsyn K, OPG, and osteocalcin. Radiographically, linear measurements showed a statistically significant reduction in bone loss after treatment with PLGA+ 10 mg/kg Met compared to the positive control ($p < 0.05$). RT-PCR showed increased *AMPK e*xpression ($p < 0.05$) and decreased expression of *NF-κB P65*, *HMGB1* and *TAK-1* after PLGA+ 10 mg/kg Met ($p < 0.05$). The PLGA nanoparticle + 10 mg/kg Met decreased glucose levels and also decreased the inflammatory response, and bone loss in ligature-induced periodontitis in rats.

Keywords: nanoparticles; poly lactic-co-glycolic acid; metformin; periodontal disease; inflammation

1. Introduction

Polymeric nanoparticles are particles with a diameter between 1 and 1000nm [1]. In recent years, nanoparticulate drug release systems using biodegradable polymers have been extensively studied for various applications [2,3]. Nanoparticles may offer advantages such as: increased therapeutic efficacy, prolonged and controlled release of the drug, decreased toxicity, as well as stability and lower drug decomposition [4,5].

Among the polymers studied for nanoparticle preparation, poly lactic-co-glycolic acid (PLGA) has been widely used because it is a biocompatible and biodegradable synthetic polymer that has been approved by the United States Food and Drug Administration (USFDA) [6].

Polymer composition is the most important factor to determine the hydrophilicity and degradation rate of a delivery matrix. The amount of glycolic acid is a critical parameter in tuning the hydrophilicity of the matrix and therefore the degradation and drug release rate [7].

Biguanides are an important class of oral hypoglycemic agents and act by inhibiting gluconeogenesis in the liver, increasing the density of low and high affinity receptors for insulin and decreasing resistance to the peripheral effects of insulin [8].

Currently, Metformin is the most commonly used oral hypoglyceminate for treating type 2 diabetes and is generally accepted as first-line treatment for this disease [9]. This treatment in diabetes patients has shown that there is reduced TNF-α expression [10], with confirmed anti-inflammatory activity [11].

The effect of metformin on periodontal disease was previously confirmed by our group, where the best bone loss results were found when metformin was administered at a dose of 50 mg/kg. The therapeutic dose of metformin in humans occurs in a range of 1700mg-3000mg/day. The dose of 50 mg/kg in rats is below the therapeutic dose (approximately 567 mg/day). However, it is important to consider that the animals in this study were not diabetic, since our objective was to verify the pleiotropic effect of Metformin in periodontal disease [12]. For this study, our investigation objective is the effect of Metformin hydrochloride-PLGA nanoparticles on diabetic rats in a periodontal disease experimental model.

2. Results

2.1. Characterization of Met-Loaded Plga Nanoparticles

The well-defined spherical morphology and smooth surface of free-drug PLGA nanoparticles and MET-loaded PLGA nanoparticles can be directly observed in AFM image (Figure. 1). Table 1 showed the mean diameter of MET-loaded PLGA nanoparticles was in a range of 457.1 ± 48.9nm with a polydispersity index of 0.285, zeta potential o 8.16 ± 1.1 mV and entrapment efficiency (EE) was 70% (Table 1). These results suggest that the addition of MET in the core slightly affected the particle sizes ($p>0.05$). The mean particle size of MET-loaded PLGA nanoparticles was a bit larger than that of pure empty PLGA nanoparticles, indicating the presence of MET in the hydrophilic core of the nanoparticles (2,3).

Peer-reviewed version available at Int. J. Mol. Sci. 2018, 19, 3488; doi:10.3390/ijms19113488

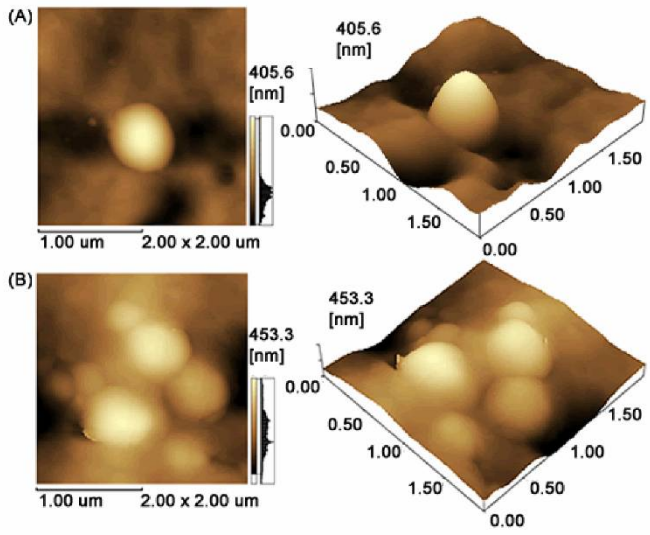

Figure 1.

Table 1. Loading efficiency of Metformin-loaded PLGA nanoparticles by double emulsification.

Formulation	Particle Size (nm)	PDI	Zeta Potential (mV)	EE (%)
NP Empty	406.3 ± 14.5	0.187 ± 0.01	-1.51 ± 3.2	-
NP + MET	457.1 ± 48.9	0.285 ± 0.12	8.16 ± 1.1	66.7 ± 3.73

Notes: PLGA, poly (lactic-co-glycolic acid); NP, nanoparticles; PDI, Polydispersity Index; MET, Metformin; EE, Encapsulation efficiency. The results are expressed as mean ± SD (n = 3).

2.2. Glucose Dosing

Induction of diabetes occurred in the control groups (DM and Positive control) and also in all treated experimental groups, and diabetes was confirmed for values greater than 300 ml/dl of blood glucose. Only treatment with PLGA+10mg/kg Met significantly reduced glucose levels in the animals (Table 2).

Table 2. Glucose levels: Sham group (unbound group), PD (bound), DM (diabetic group without ligation), DM + PD (diabetic group and with ligation), Met 50 (group bound and treated with MET 50 mg/kg), Met100 (bound and treated group with MET 100 mg/kg) and Met 200 (bound and treated group with MET 200 mg/kg), PLGA + 100 mg/kg Met 100 mg/kg + PLGA) PLGA + 10mg/kg Met (group bound and treated with MET 10mg/kg + PLGA).

Groups	Glucose mg/dL (Mean + Standard deviation)
Sham	115.7 ± 18.86 [a ***, b ***]
PD	176.7 ± 90.4 [a ***, b ***]
DM	605 ± 52.16
Positive control/PD+DM	529.9 ± 76.78
Met 50	523.2 ± 31.74
Met 100	522.0 ± 78.32
Met 200	454.3 ± 59.9
PLGA + 10mg/kg Met	286.5 ± 129.6
PLGA + 100mg/kg Met	440 ± 59.9 [a ***, b ***]

a= Difference among groups and DM, b= difference among groups and Positive control/DP+DM, ***p<0.001.

Peer-reviewed version available at Int. J. Mol. Sci. 2018, 19, 3488; doi:10.3390/ijms19113488

2.3. Histopathological Analysis

Histopathological data for the Sham and DM control groups showed that infiltration of inflammatory cells was absent or scarce and was restricted to the marginal gingival region, and that the alveolar bone and cement were preserved with scores 0 (0-0) for both groups; the difference being significant when compared to the PD and Positive control groups ($p < 0.001$), figure 2 and 3 . The PD and positive control groups presented scores of 2.8 (2.5-3.0) and 3 (3-3), respectively, with presence of marked infiltration of inflammatory cells in the gingiva and periodontal ligament, marked degradation of the alveolar bone, and partial to severe destruction of dental cement, figure 2 and 3. The experimental groups Met 50, score: 3 (1.5-3), Met 200, Score: 3 (2.25-3) and PLGA + 100mg/kg Met, Score 3 (2-3) showed a marked inflammatory infiltrate in the gingiva and periodontal ligament, marked degradation of the alveolar process and partial to severe destruction of the cement. In turn, the experimental groups Met 100, score: 2 (1.5-3) indicated marked cellular infiltration in the gingiva and periodontal ligament, moderate degradation of the alveolar process and low cementation, figure 2 and 3. On the other hand, the PLGA + 10mg/kg Met, score 2 (1.5-2.5) group indicated moderate inflammatory cellular infiltrate throughout the gingival insertion, light alveolar resorption, and intact cement, with a significant reduction in bone loss when compared to the positive control group ($p < 0.05$), figure 2 and 3.

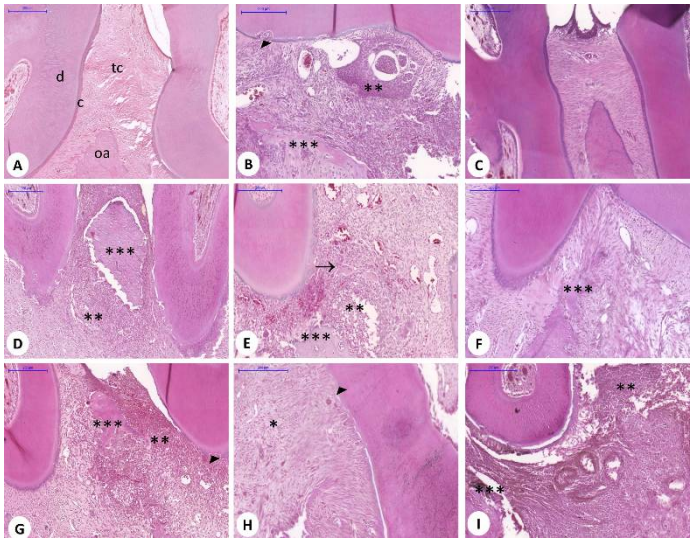

Figure 2.

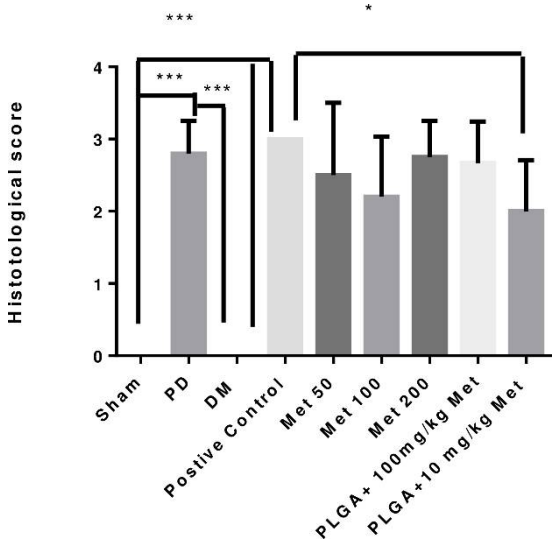

Figure 3.

Peer-reviewed version available at Int. J. Mol. Sci. 2018, 19, 3488; doi:10.3390/ijms19113488

134 *2.4. Cytokines*

135 The quantification of inflammatory cytokines showed a significant reduction of IL-1 beta and
136 TNF-alpha in the Sham group when compared to the positive control group ($p < 0.001$). The treatment
137 PLGA + 10mg/kg Met significantly reduced the IL-1 Beta and TNF-alpha levels ($p < 0.05$), figure 4.

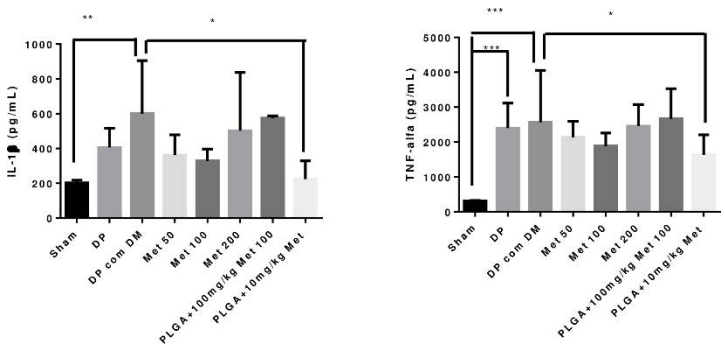

138

139 **Figure 4.**

140 *2.5. RT-PCR*

141 Quantification of gene expression for the inflammatory NFKB p65 transcription factor showed
142 a significant reduction for the Sham and PLGA + 10mg/kg Met groups ($p < 0.05$), figure 5. A
143 transcription factor directly related to the action mechanism of metformin is activated protein kinase
144 (AMPK). AMPK provides a target capable of mediating the beneficial metabolic effects of metformin.
145 AMPK is a key for metabolic enzymes such as 3-hydroxy-3-methylglutaryl CoA reductase (HMGCoA
146 reductase). Quantification of the gene expression of AMPK showed a significant increase in this
147 transcription factor for diabetic animals and periodontal disease treated with PLGA + 10mg/kg Met
148 when compared to the positive and PLGA + 100mg/kg Met ($p < 0.05$) groups, figure 5. HMGB1, a
149 nuclear protein released from activated macrophages or injured cells, displays pro-inflammatory
150 cytokine-like properties once it enters the extracellular space and HMGB1-induced
151 osteoclastogenesis. Quantification of the HMGB1 gene expression showed a significant reduction for
152 the Sham and PLGA + 10mg/kg Met groups ($p < 0.05$) when compared to the positive control, figure
153 5. TAK1 is indispensable to RANKL-induced osteoclastogenesis. The quantification of gene
154 expression showed a significant reduction for the Sham and PLGA + 10mg/kg Met groups ($p < 0.05$)
155 when compared to the positive control, figure 5.

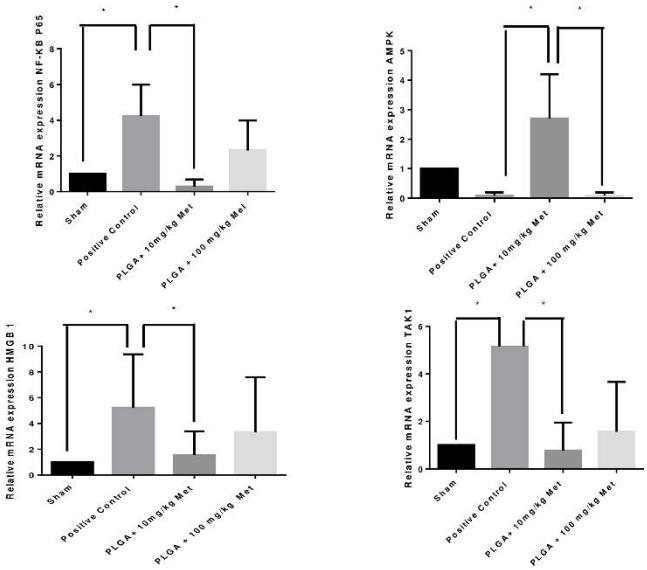

156

157 **Figure 5.**

Peer-reviewed version available at Int. J. Mol. Sci. 2018, 19, 3488; doi:10.3390/ijms19113488

158 *2.6. Radiographic Assessment of Alveolar Bone Loss*

159 Rats with PD + DM (Positive control) (0.97mm ± 0.35mm), showed statistically significant more
160 linear bone loss compared to Sham (0.45 mm ± 0.08mm), $p<0.05$. However, when comparing Positive
161 control (0.97mm ± 0.35mm) to PLGA 10 mg/kg Met (0.48 ± 0.14mm) treatment, bone loss was reduced.
162 PLGA + 100 mg/kg Met showed bone loss (0.81 mm ± 0.28mm) (Figure 6).

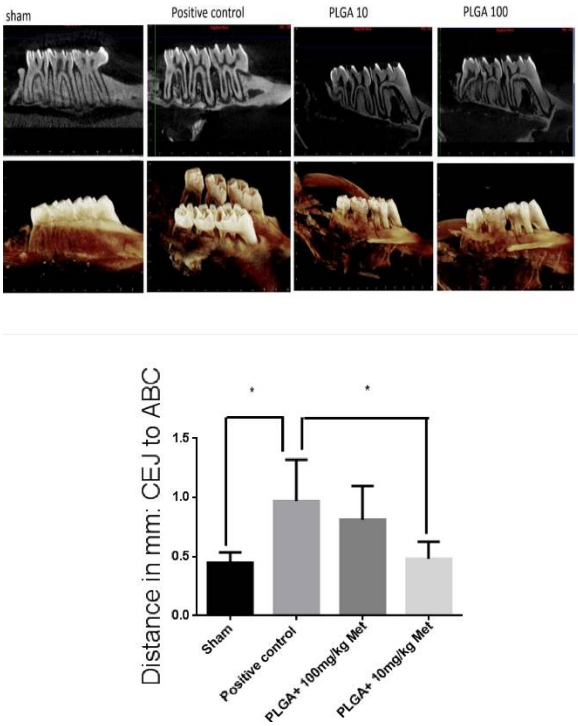

163
164 **Figure 6.**

165 *2.7. Immunohistochemistry*

166 The sham group showed immunostaining absence for RANK, RANKL, OPG and cathepsyn, and
167 low staining for osteocalcin. The positive control group showed intense immunostaining for RANKL
168 and Cathepsyn, more significantly than Sham group ($p < 0.001$) and the PLGA+ 10 mg/kg group
169 ($p<0.05$). The PLGA+ 10 mg/kg Met treatment resulted in low staining of RANKL, OPG,
170 Osteocalcin, Cathepsin and osteocalcin (Figure 7 and 8).

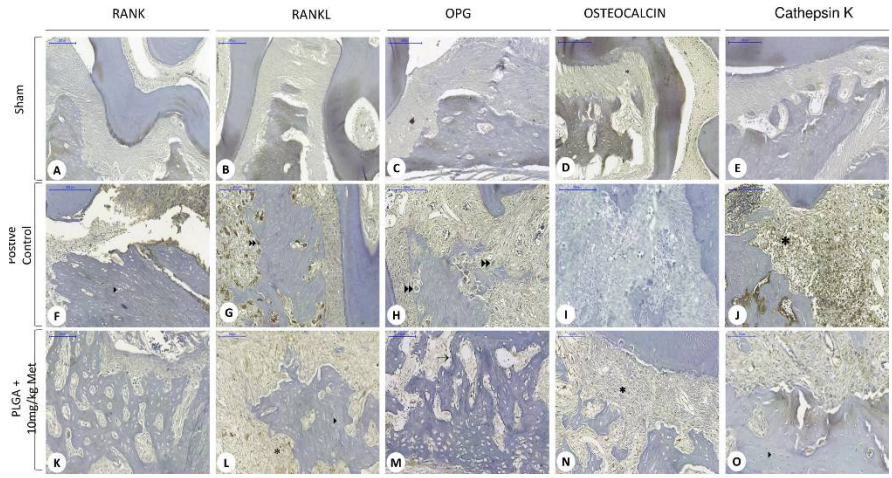

171
172 **Figure 7.**

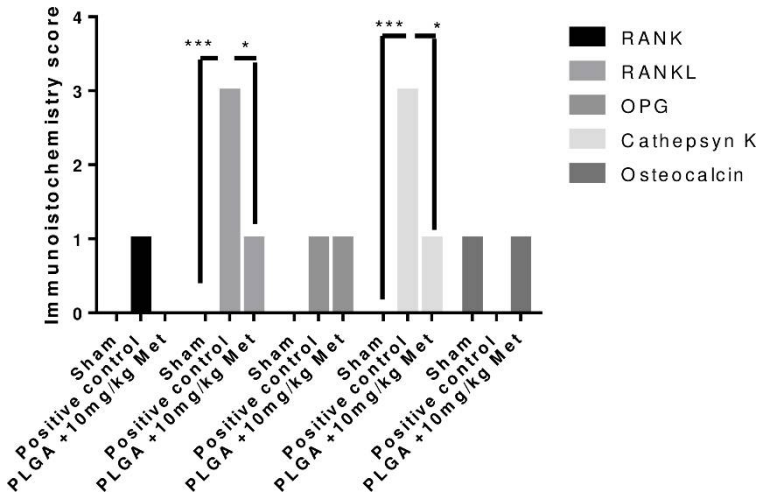

Figure 8.

3. Discussion

Poly lactic acid contains an asymmetric α-carbon which is typically described as the D or L form in classical stereochemical terms. The enantiomeric forms of the polymer PLA are poly D-lactic acid (PDLA) and poly L-lactic acid (PLLA). PLGA is generally an acronym for poly D,L-lactic-*co*-glycolic acid, where D- and L- lactic acid forms are in equal ratio [7]. PLGA can be processed into almost any shape and size, and can encapsulate molecules of virtually any size. The mechanical strength of PLGA is affected by physical properties such as molecular weight and polydispersity index [7]. These properties also affect the ability to be formulated as a drug delivery device and may control the device degradation rate and hydrolysis. When co-polymerized with PLA, crystalline PGA reduces the crystallinity degree of PLGA and as a result increases the hydration and hydrolysis rates. As a rule, higher PGA content leads to quicker degradation rates with an exception of a 50:50 ratio of PLA/PGA, which exhibits the fastest degradation with higher PGA content leading to an increased degradation interval below 50 [13]. In this study, MET-loaded PLGA nanoparticles with a 50:50 ratio was in the range of 457.1 ± 48.9nm with a polydispersity index of 0.285, zeta potential of 8.16 ± 1.1 mV and entrapment efficiency (EE) was 70%. These results suggest that the addition of MET in the core slightly affected the particle sizes.

Our data showed that the association of metformin with PLGA was able to reduce glucose levels of 529.9 dl/ml^3 (positive control group) to 286. 5 dl/ml^3 (MET 10 + PLGA group), although used in rats at a 10X lower dose to the dose considered within the range used in humans [12], demonstrating that the incorporation of drugs into nanoparticles may have a low polydispension index [14]. A low polydispersion coefficient guarantees greater control in the drug release, in addition to being more stable during storage in biological fluids [7]. These results indicate that incorporation of the drug into the nanoparticle has systemic benefits, thus favoring glycemia control with a dose reduction of metformin, which reduces the adverse effects.

PLGA is the most successful and most featured polymer for drug-controlled release systems. It is favored because of its biocompatibility, biodegradability and mechanical strength, and is still being used to develop new controlled release systems [15]. The effects of the combination of metformin and PLGA can be observed in both the inflammatory process and in the reduction of bone loss in periodontal disease. The histopathological findings show a reduction of the inflammatory infiltrate, little destruction of the periodontal ligament and absence of dental cement impairment in the group treated with metformin at the dose of 10 mg/kg + PLGA.

This association showed excellent results in periodontal disease in diabetic animals; clinical and histopathological data corroborate the findings that elucidate the main cellular and molecular mechanisms involved in controlling inflammation and bone loss in periodontal disease.

In general, drugs are small enough molecules to cross the endothelium in almost all regions of the body after systemic administration, and can reach both target regions and other healthy regions

Peer-reviewed version available at Int. J. Mol. Sci. 2018, 19, 3488; doi:10.3390/ijms19113488

not affected by any disease, thus causing associated side effects of medication. The use of colloidal nanoparticle systems helps to control these adverse effects and improves therapeutic efficacy. These drugs are encapsulated within nanoparticles of 50-800nm, which are not able to cross the vessel wall of healthy regions of the body (the space between these cells is only 15-30nm) [16]. Nanoformulation also demonstrates increased anti-inflammatory effects and drug retention at the action site [17]. The present study showed that all groups treated with metformin significantly reduced the inflammatory markers (IL-1 beta and TNF-alpha) with a prominence of MET 10 mg/kg + PLGA.

The RANKL, RANK and OPG system represents the key molecular regulation for bone remodeling [18]. Studies have shown a favorable effect of Metformin on bone formation. There are two action mechanisms suggested for the osteogenic effect of Metformin, which are: increased osteoblast proliferation and decreased osteoclast activity. Studies indicate that the proliferation of Metformin is increased after its absorption by osteoblasts [19]. This drug negatively regulates RANKL production and positively regulates osteoprotegerin (OPG) production from osteoblasts [20]. Thus, there is a decrease in osteoclast activity through this decrease in the RANKL/OPG ratio, aiding in inducing bone formation and inhibiting resorption [21]. In our study it was found in vivo that metformin at the dose of 10mg/kg + PLGA reduced bone loss with increased osteocalcin immunoblotting and reduced RANKL, indicating an increase in mature osteoblasts and a reduction in the number of osteoclasts.

AMP-activated protein kinase (AMPK) has emerged as a detection mechanism in regulating cellular energy homeostasis and is an essential mediator of the central and peripheral effects of many hormones in glucose metabolism [22]. It is a key molecule in controlling metabolic diseases such as type 2 diabetes and obesity, and is activated by antidiabetic drugs such as metformin and thiazolidinediones [23]. Most isoforms of AMPK subunits are expressed in bone cells and bone tissue. It was observed *in vitro* that metformin (50 μM) significantly increased the expression of osteocalcin, stimulated alkaline phosphatase activity and increased cell mineralization, yet significantly activated AMPK in dose and time-dependent forms [24]. AMPK plays a critical role as a negative feedback regulator of RANKL's osteoclast formation promoting action [25]. Araújo et al. (2017) [12] demonstrated that a low dose of metformin reduced bone loss, decreased RANKL and increased relative expression of AMPK mRNA. Osteocalcin is specifically expressed in osteoblasts, secreted in circulation, and can regulate glucose homeostasis. Metformin stimulates the expression of osteocalcin and the differentiation of osteoblasts via AMPK activation [24]. In our study it was observed that MET 10mg/kg + PLGA activated AMPK gene expression which led to a stimulus of osteocalcin expression and consequently osteoblast deposition and bone formation.

Lee et al. 2010 [25] demonstrated that AMPK acts via CaMKK and TAK1 activation to serve as a negative feedback regulator of RANKL-induced osteoclast formation. Mizukami et al. [26] also reported that RANKL stimulation facilitates the formation of a complex containing RANK, TRAF6, TAB2 and TAK1, leading to the activation of TAK1. RANKL also acts through TRAF6 to activate TAK1, promoting osteoclastogenesis via NF-k beta activation. More interestingly, CaMKK and TAK1 can be activated by RANKL in osteoclast precursors.

HMGB1 acts by stimulating the differentiation of osteoclast precursors in the presence of RANKL and has similar proinflammatory properties to cytokines once it enters the extracellular space [27]. Thus, in our study we were able to observe a reduction in HMGB1 at the dose of MET 10 mg/kg, thus showing its relation with inflammation control and in bone loss, since it contributed to decrease the NFK beta and RANKL levels.

This study showed that the PLGA + 10mg/kg Met association had better results, as it managed to control blood glucose levels below what is considered as diabetes, and so this nanotechnology product guaranteed rational release of the drug at the inflammation site, thereby controlling inflammation and bone loss in the experimental periodontal disease model.

4. Material and Methods

Metformin hydrochloride was purchased from Companhia da Fórmula D, L-PLGA 50:50 (inherent viscosity of 0.63 dL g^{-1} at 30°C) was purchased from Birmingham Polymers Inc. (USA),

Peer-reviewed version available at Int. J. Mol. Sci. 2018, 19, 3488; doi:10.3390/ijms19113488

Polyvinyl alcohol (PVA) was purchased from Sigma-Aldrich Co. (St. Louis, MO, USA), and dichloromethane (DCM) from QHEMIS® (Brazil). Purified water (1.3 μS.cm^{-1}) was prepared from reverse osmosis purification equipment, (OS50 LX Gehaka, São Paulo, Brazil). All other reagents were of analytical grade.

4.1. Experimental Design and Preparation of MET-loaded PLGA Nanoparticles

PLGA nanoparticles for metformin encapsulation were fabricated by adapting the double emulsion solvent diffusion technique [28-30] with some modifications: 50 mg of PLGA was dissolved in 6 ml of *Dichloromethane* (DCM). Metformin (272 mg/mL) was dissolved in an aqueous phase containing 0.1% polyvinyl alcohol. The aqueous phase with the drug (600 μL) was added into 3 mL of organic phase containing PLGA. The mixture was emulsified with a probe-tip sonicator (probe-tip diameter: 1.3 cm, Sonics &Materials Inc., Danbury, CT, USA) operating at 50% amplitude intensity for 1 minute. This first mixture was then added into 6 mL of water containing 1.0% of PVA and the mixture was emulsified with a probe-tip sonicator for 1 minute. This emulsion was added into 8 mL of water containing 1.0% PVA under magnetic stirring, leading to the formation of a W/O/W emulsion with MET-loaded PLGA nanoparticles. The organic solvent was allowed to evaporate overnight by stirring over a magnetic stir plate. Free-drug nanoparticles were prepared using the same procedure but excluding the drug.

4.2. Physicochemical Aspects

Mean diameter and particle size distribution were carried out by dynamic light scattering in a ZetaPlus device (Brookhaven Instruments Co., USA) equipped with a 90Plus/BI-MAS apparatus at a wavelength of 659 nm with a scattering angle of 90º. Zeta potential of the particles was measured by laser Doppler anemometry using the same equipment. All analyses were performed at 25ºC. Experimental values were given as the mean ± SD for the experiments and carried out in triplicate for each sample. The shape and surface of drug-free and MET-loaded nanoparticles were observed using AFM images. The dispersions were freshly diluted with purified water at a ratio of 1:25 (v/v) and dropped in a cover slip, dried under a desiccator for 24 h and then analyzed in a Shimadzu SPM-9700 AFM (Tokyo, Japan) at room temperature with a cantilever in non-contact mode at 1Hz scanning. Samples were prepared by using one drop of dispersion, which was placed on a washed microscope slide and dried under a desiccator for 24 h and then analyzed at 25ºC in a cantilever in non-contact mode.

4.3. Drug Loading Efficiency

PLGA nanoparticles were used in this experiment to obtain an efficient drug loading corresponding to 6mg/mL. MET loading was assessed by indirect method in which dispersions were centrifuged at 16,900 RCF (g) per 60 min at 4ºC using an ultra-centrifugal filter (Sartorius®, Vivaspin 2, Ultra-15 MWCO 10 kDa). The supernatant was removed and diluted in purified water 1:20 (v/v) and the measurements were carried out in a UV Thermo Fisher Scientific 60S Evolution Spectrophotometer (USA), using previously validated UV spectrophotometry at 232 nm. Entrapment efficiency (EE) was calculated using the following equation: EE% = (total drug – drug determined in the supernatant)/total drug x 100.

4.4. In Vivo Experimental Study (Periodontal Disease Experimental Model)

The experiments were performed on male Wistar rats (180–220 g) housed under standard conditions (12 h light/dark, 22 ± 0.1°C), with ad libitum access to food and water. All animal protocols were approved by the Animal Ethics Committee of the Federal University of Rio Grande do Norte, Brazil. The anesthesia used to induce periodontal disease by intraperitoneal administration was Ketamine 10% (70 mg/kg, Vetnil, São Paulo, Brazil) and 2% xylazine (10 mg/kg, São Paulo, Brazil). The animals were euthanized with 80 mg/kg thiopental, followed by cervical dislocation (Cristália, São Paulo, Brazil).

Peer-reviewed version available at Int. J. Mol. Sci. 2018, 19, 3488; doi:10.3390/ijms19113488

4.5. Control and Experimental Groups

Control Groups:

20 animals without diabetes and without periodontal disease (Sham)

20 animals with periodontal disease and without diabetes (PD)

20 animals with diabetes and without periodontal disease (DM)

20 animals with diabetes and with periodontal disease (positive Control/PD + DM)

Experimental groups: Metformin hydrochloride

20 animals with diabetes and with periodontal disease and Metformin 50 mg/kg/day DOSE (Met 50)

20 animals with diabetes and periodontal disease and Metformin 100 mg/kg/day DOSE (Met 100)

20 animals with diabetes and periodontal disease and Metformin 200 mg/kg/day DOSE (Met 200)

Experimental groups: Metformin hydrochloride-PLGA nanoparticles

From the best histopathological results, 02 experimental groups were defined for Metformin hydrochloride-PLGA nanoparticle association (with periodontal disease and diabetes). The best anti-inflammatory dose of Metformin was used and a lower 10X dose of metformin was used.

20 animals with diabetes and periodontal disease and 100 mg/kg/day of Metformin + PLGA (PLGA + 100 mg/kg Met)

20 animals with diabetes and with periodontal disease and 10 mg/kg/day DOSE of Metformin + PLGA (PLGA + 10 mg/kg Met)

4.6. Diabetes Induction

Diabetes was induced by administration of Streptozotocin/STZ (Sigma Aldrisch) (40 mg/kg, ip) through the penile vein, dissolved in Sodium Citrate buffer (0.01M, pH 4.5) at the concentration of 40mg/kg body weight under general anesthesia with 3% isoflurane inhalation. After one week of STZ administration, glucose was measured by a glycosometer (One touch select simple). Upon reaching plasma glucose stability of ≥300 mg/dL, the animals were considered diabetic and selected for later Periodontal Disease studies. A puncture was made in the initial portion of the animal's tail using a sterile needle and the blood was collected on a reagent strip for glucose determination.

4.7. Periodontal Disease Induction

After diabetes confirmation, Periodontal Disease induction was performed by placing a 3.0 nylon wire on the second left molar of male Wistar rats with the animals under i.p. ketamine (80mg/kg) and xylazine (10mg/kg) anesthesia. Oral treatments were performed by gavage 30 minutes prior to periodontal disease induction, which continued until the 10th day. Euthanasia by thiopental (80 mg/kg) was performed on the 11th day. After sacrificing the animals, the gingival and maxillary tissue samples were sent for analysis.

4.8. Histopathological Analysis (Decalcified Tissue)

Histological analyzes were independently performed by two calibrated pathologists. All groups (controls and experimental) were analyzed by histopathology. This step selected the best results that were used for the subsequent analyzes. The sectioning was performed in the morphology laboratory of the UFRN, and the slides were analyzed by light microscopy in the Department of Morphology. Five jaws were used per group. Alveolar bone specimens were collected, fixed in 10% buffered neutral formol, and demineralized in 5% nitric acid. The samples were then dehydrated, embedded in paraffin and sectioned along the molars in the mesiodistal plane for hematoxylin and eosin. Sections (4 μm) corresponded to the area between the first and second maxillary molars where ligation was placed for analysis by light microscopy (40 × magnification). Influx of inflammatory cells and alveolar bone integrity and cement were analyzed. A score of 0 indicated that infiltration of inflammatory cells was absent or scarce and was restricted to the marginal gingival region, and that

Peer-reviewed version available at Int. J. Mol. Sci. 2018, 19, 3488; doi:10.3390/ijms19113488

the alveolar process and cement were preserved; a score of 1 indicated moderate cell infiltration throughout the gingival insert, minor alveolar resorption, and intact cement; a score of 2 indicated marked cellular infiltration in the gingiva and periodontal ligament, marked degradation of the alveolar process and partial destruction of the cement; and 3 indicated marked cellular infiltration, complete reabsorption of the alveolar process and severe destruction of the cement.

4.9. Elisa immunoassay for Detection of IL-1β and TNF-α

Gingival tissues (n = 5) of the control (Sham, PD and Positive control) and experimental groups were stored at -70°C. IL-1β levels (detection range: 62.5-4000 pg/mL; lower detection limit: 12.5 ng / ml of recombinant mouse IL-1β) and TNF-α (detection range: 62.5-4000 pg/ml; lower limit of detection: 50 ng / ml mouse TNF-α recombinant) were determined using commercial ELISA kits (R & D Systems, Minneapolis, MN, USA) as previously described [15]. All samples were measured at 490 nm.

First, microtiter plates were coated overnight at 4°C with rat antibodies against TNF-α, IL-1β, and IL-10. Plates were then blocked, samples and standards added in several dilutions, in duplicate and incubated at 4°C for 24 h. The plates were washed three times with buffer and the antibodies added to the wells (anti-TNF-α, anti-IL-1β, or anti-IL-10 sheep biotinylated polypropylene, diluted 1000 with 1% BSA assay buffer). Plates were incubated at room temperature for 1 hour, washed, and 50 ul of avidin-HRP (1 5000) were added. Then o-phenylenediamine reagent coloring (50 mL) was added 15 min later, and the plates were incubated in the dark at 37 °C for 15-20 min. The enzymatic reaction was reduced with H_2SO_4 and the absorbance measured at 490 nm. Values were expressed in pg/mL.

4.9.1. Genetic Marker Rt-Pcr Analysis for Periodontal Disease in Diabetic Animals

The control (sham and positive control) and experimental groups (PLGA + 100mg / kg Met and PLGA + 10mg / kg met) were included in the quantification of expression by RT-PCR. Total RNA from the gingival tissues of the treated groups were extracted using the Trizol reagent (Invitrogen, Carlsbad, CA, USA) according to the manufacturer's guidelines and stored at –70 °C.

RNA concentration was determined from the optical density at a wavelength of 260 nm (using an OD_{260} unit equivalent to 40 μg/ml RNA). Five micrograms of isolated total RNA were reverse transcribed to cDNA in a reaction mixture containing 4 μl 5X reaction buffer, 2 μl dNTP mixture (10 mM), 20 units of RNase inhibitor, 200 units of avian-myeloblastosis virus (AMV) reverse transcriptase, and 0.5 μg oligo(dT) primer (High-Capacity cDNA Reverse Transcription Kit, Foster City, USA) in a total volume of 20 μl. The reaction mixture was incubated at 42 °C for 60 min, and the reaction was terminated by heating at 70 °C for 10 min. The cDNA was stored at –80 °C until further use. Gene expression was evaluated by PCR amplification using primer pairs based on published rat sequences (GADPH- Rattus norvegicus: Forward primer: AACTTGGCATCGTGGAAGG, Reverse Primer: GTGGATGCAGGGATGATGTTC; AMPK-Rattus norvegicus protein kinase, AMP-activated, alpha 2 catalytic subunit (Prkaa2), mRNA: Forward primer: AGCTCGCAGTGGCTTATCAT, Reverse Primer: GGGGCTGTCTGCTATGAGAG; NF-κB-Rattus norvegicus v-rel avian reticuloendotheliosis viral oncogene homolog A (Rela), mRNA Forward primer: TCTGCTTCCAGGTGACAGTG, Reverse Primer: ATCTTGAGCTCGGCAGTGTT; Hmgb1-Rattus norvegicus high mobility group box 1 (Hmgb1), mRNA: Forward primer: GAGTACCGCCCAAAAATCAA, Reverse Primer: TTCATCCTCCTCGTCGTCTT; TAK-1 Forward primer:: GTCATCCAGCCCTAGTGTCAGATT, Reverse Primer: TTCTTTGGAGTTTGGGCACG. Transforming Growth Factor β-activated Kinase 1 TAK1- Mus musculus, mRNA: Forward primer: GTC ATC CAG CCC TAG TGT CAG AAT, Reverse Primer: TTC TTT GGA GTT TGG GCA CG-3′

Quantitative RT-PCR was performed using Power SYBR Green master mix (Applied Biosystems, USA), and a Step One Plus thermocycler (Applied Biosystems, USA), according to the manufacturer's instructions. For the 1X PCR master mix, 2.5 μl of each cDNA was added in a final volume of 20 μl. The PCR conditions were as follows: 95 °C for 5 min, 40 cycles of 30 s at 95 °C, 30 s at 52–60 °C (based on the target), and 60 s at 72 °C. The relative quantitative fold change compared with the control

Peer-reviewed version available at Int. J. Mol. Sci. 2018, 19, 3488; doi:10.3390/ijms19113488

(Sham) was calculated using the comparative Ct method, where Ct is the cycle number at which fluorescence first exceeds the threshold. The Ct values from each sample were obtained by subtracting the values for GADPH Ct from the target gene Ct value. The specificity of resulting PCR products was confirmed by melting curves.

4.10. Radiographic Micro-Computed Tomography (Microct) Measurement of Abl

In this stage, the control groups (Sham and positive control) and experimental groups (PLGA + 100mg/kg Met and PLGA + 10mg/kg met) were included. Animals were euthanized at the end of the experiment (10 days after addition of the ligature and first drug treatments); maxillae were dissected and fixed in 10% buffered formalin for 24 hours and stored in 70% alcohol. Rat maxillae were scanned using micro-computed tomography (μCT, micro-CT) (Model 1172; SkyScan, Kontich, Belgium) at 20 micrometers resolution. Micro-CT files were converted to Digital Imaging and Communications in Medicine (DICOM) files and imported into Dolphin® software for linear bone height analysis. Linear bone height analysis was performed by positioning the second molar cementoenamel junctions (CEJ) parallel to each other in the coronal plane. In the axial plane, the middle of the crown was identified and linear bone distances were recorded on the mesial aspect of the second molar on the sagittal image. Additional measurements were taken 0.3mm palatal from the middle of the crown, again recording the mesial aspect of the second molar on the sagittal image. The linear measurements were recorded from the CEJ to the alveolar crest (AC). Each second molar received a total of 2 measurements, and these values were averaged for each group. Samples were positioned using DataViewer (V.1.5.2 Bruker, Billerica, MA) such that the CEJ's of the second molar were parallel to each other in the sagittal and coronal planes in order to assess volumetric bone volume/tissue volume (BV/TV) changes. The axial plane showed the first, second, and third crowns of each molar. The images were analyzed using CTAn (V.1.16 Bruker, Billerica, MA). A 40-slice volume set at a threshold of 75 in the bifurcation area of the second molar was used as a region of interest for analysis (n≥3/group for all μCT analysis).

4.11. Immunohistochemistry

Only controls (Sham and positive control) and experimental group (PLGA + 10 mg/kg met) were included in this step. Fine sections of periodontal tissue (4 μm) (3 mandibles per group) were produced using a microtome and transferred onto gelatin coated slides. Each section was deparaffinized and rehydrated. Gingival and periodontal tissues were washed with 0.3% Triton X-100 in phosphate buffer, then extinguished with peroxidase (3% hydrogen peroxide) and incubated with the following primary antibodies (Santa Cruz Biotechnology, Interprise, Brazil) overnight at 4°C: RANKL, 1400; OPG, 1400; cathepsin K, 1400; and osteocalcin, 1400, which were washed with phosphate buffer and incubated with streptavidin-HRP-conjugated secondary antibodies (Biocare physicians, Concord, CA, USA) for 30 minutes, and immunoreactivity for RANK, RANK-L, OPG, cathepsin K and osteocalcin were visualized using a colorimetric detection kit following the manufacturer's instructions (TrekAvidin-HRP Label + Kit, Biocare , Dako, USA).

Statistical analysis

Using the nanoparticle characterization, pairwise comparisons of the analytical data were performed using the Student's t-test. One-way analysis of variance (ANOVA) was applied for multiple comparisons, followed by Tukey's post hoc test. $P<0.05$ was considered statistically significant. Data for the *in vivo* experiments were analyzed using descriptive and analytical statistics. Parametric tests such as ANOVA, followed by Bonferroni's post-test and non-parametric Kruskall-wallis test were used. A significance level of 5% was considered.

Author Contributions: Conceptualization, de Sousa Barbosa Freitas Pereira, Gerly Anne de Castro Brito and Aurigena Antunes de Araújo; Data curation, Gerly Anne de Castro Brito and Aurigena Antunes de Araújo; Formal analysis, Gerly Anne de Castro Brito and Aurigena Antunes de Araújo; Funding acquisition, Aurigena Antunes de Araújo; Investigation, de Sousa Barbosa Freitas Pereira, Maria Laura de Souza Lima, Arnóbio

Antônio da Silva Júnior, Emanuell dos Santos Silva, Adriana Augusto de Rezende, Raul Hernandes Bortolin, Maria Galvan, Flavia Q Pirih, Raimundo Fernandes de Araújo Júnior, Caroline Addison Carvalho Xavier de Medeiros, Gerlane Coleho Bernando Guerra and Aurigena Antunes de Araújo; Methodology, de Sousa Barbosa Freitas Pereira, Maria Laura de Souza Lima, Arnóbio Antônio da Silva Júnior, Emanuell dos Santos Silva, Adriana Augusto de Rezende, Raul Hernandes Bortolin, Maria Galvan, Flavia Q Pirih, Raimundo Fernandes de Araújo Júnior, Caroline Addison Carvalho Xavier de Medeiros, Gerlane Coleho Bernando Guerra and Aurigena Antunes de Araújo; Project administration, Aurigena Antunes de Araújo; Supervision, Gerly Anne de Castro Brito, Flavia Q Pirih, Raimundo Fernandes de Araújo Júnior and Aurigena Antunes de Araújo; Validation, de Sousa Barbosa Freitas Pereira; Visualization, Aurigena Antunes de Araújo; Writing – original draft, de Sousa Barbosa Freitas Pereira and Aurigena Antunes de Araújo; Writing – review & editing, de Sousa Barbosa Freitas Pereira and Aurigena Antunes de Araújo

Funding: This study was supported by the *Conselho Nacional de Desenvolvimento Científico e Tecnológico* (*CNPq*; 401838/2016-1).

Conflicts of Interest: The authors declare no conflict of interest.

Abbreviations

PLGA	Poly (D, L-Lactide-co-glycolide)
NPs	Nanoparticles
Met	Metformin
AFM	Atomic force microscopy
μCT	Micro-computed Tomography

References

1. Freichels, H.; Danhier, F.; Préat, V.; Lecomte, P.; Jérôme, C. Fluorescent labeling of degradable poly(lactide-co-glycolide) for cellular nanoparticles tracking in living cells. *The International Journal Of Artificial Organs* **2011**, *34*, 152-160.
2. Jia, L. Nanoparticle formulation increases oral bioavailability of poorly soluble drugs: Approaches experimental evidences and theory. *Current nanoscience* **2005**, *1*, 237-243.
3. Lai, F.; Schlich, M.; Pireddu, R.; Corrias, F.; Fadda, A.M.; Sinico, C. Production of nanosuspensions as a tool to improve drug bioavailability: Focus on topical delivery. *Current pharmaceutical design* **2015**, *21*, 6089-6103.
4. Sharma, A.; Madhunapantula, S.V.; Robertson, G.P. Toxicological considerations when creating nanoparticle based drugs and drug delivery systems? *Expert opinion on drug metabolism & toxicology* **2012**, *8*, 47-69.
5. Liu, K.C.; Yeo, Y. Extracellular stability of nanoparticulate drug carriers. *Archives of pharmacal research* **2014**, *37*, 16-23.
6. Zhou, Y.; Zhang, L.; Zhao, W.; Wu, Y.; Zhu, C.; Yang, Y. Nanoparticle-mediated delivery of tgf-beta1 mirna plasmid for preventing flexor tendon adhesion formation. *Biomaterials* **2013**, *34*, 8269-8278.
7. Makadia, H.K.; Siegel, S.J. Poly lactic-co-glycolic acid (plga) as biodegradable controlled drug delivery carrier. *Polymers* **2011**, *3*, 1377-1397.
8. Kobayashi, M.; Yamazaki, K.; Hirao, K.; Oishi, M.; Kanatsuka, A.; Yamauchi, M.; Takagi, H.; Kawai, K. The status of diabetes control and antidiabetic drug therapy in japan--a cross-sectional survey of 17,000 patients with diabetes mellitus (jddm 1). *Diabetes research and clinical practice* **2006**, *73*, 198-204.
9. Bucher, S.; Bauduceau, B.; Benattar-Zibi, L.; Bertin, P.; Berrut, G.; Corruble, E.; Danchin, N.; Delespierre, T.; Derumeaux, G.; Doucet, J., *et al.* Primary care management of non-institutionalized elderly diabetic patients: The s.Ages cohort - baseline data. *Primary care diabetes* **2014**.
10. Andrews, M.; Soto, N.; Arredondo, M. [effect of metformin on the expression of tumor necrosis factor-alpha, toll like receptors 2/4 and c reactive protein in obese type-2 diabetic patients]. *Revista medica de Chile* **2012**, *140*, 1377-1382.
11. Koh, S.J.; Kim, J.M.; Kim, I.K.; Ko, S.H.; Kim, J.S. Anti-inflammatory mechanism of metformin and its effects in intestinal inflammation and colitis-associated colon cancer. *Journal of gastroenterology and hepatology* **2014**, *29*, 502-510.
12. de Araújo, A.A.; Pereira, A.d.S.B.F.; de Medeiros, C.A.C.X.; Brito, G.A.d.C.; Leitão, R.F.d.C.; Araújo, L.d.S.; Guedes, P.M.M.; Hiyari, S.; Pirih, F.Q.; de Araújo Júnior, R.F. Effects of metformin on

inflammation, oxidative stress, and bone loss in a rat model of periodontitis. *PloS one* **2017**, *12*, e0183506.

13. Miller, R.A.; Brady, J.M.; Cutright, D.E. Degradation rates of oral resorbable implants (polylactates and polyglycolates): Rate modification with changes in pla/pga copolymer ratios. *Journal of biomedical materials research* **1977**, *11*, 711-719.
14. Seijo, B.; Fattal, E.; Roblot-Treupel, L.; Couvreur, P. Design of nanoparticles of less than 50 nm diameter: Preparation, characterization and drug loading. *International journal of pharmaceutics* **1990**, *62*, 1-7.
15. Hines, D.J.; Kaplan, D.L. Poly (lactic-co-glycolic acid) controlled release systems: Experimental and modeling insights. *Critical reviews in therapeutic drug carrier systems* **2013**, *30*, 257-276.
16. Vieira, D.B.; Gamarra, L.F. Advances in the use of nanocarriers for cancer diagnosis and treatment. *Einstein (São Paulo)* **2016**, *14*, 99-103.
17. Leonard, F.; Ali, H.; Collnot, E.M.; Crielaard, B.J.; Lammers, T.; Storm, G.; Lehr, C.M. Screening of budesonide nanoformulations for treatment of inflammatory bowel disease in an inflamed 3d cell-culture model. *Altex* **2012**, *29*, 275-285.
18. Walsh, M.C.; Choi, Y. Biology of the rankl–rank–opg system in immunity, bone, and beyond. *Frontiers in immunology* **2014**, *5*, 511.
19. Bak, E.J.; Park, H.G.; Kim, M.; Kim, S.W.; Kim, S.; Choi, S.H.; Cha, J.H.; Yoo, Y.J. The effect of metformin on alveolar bone in ligature-induced periodontitis in rats: A pilot study. *Journal of periodontology* **2010**, *81*, 412-419.
20. Liu, L.; Zhang, C.; Hu, Y.; Peng, B. Protective effect of metformin on periapical lesions in rats by decreasing the ratio of receptor activator of nuclear factor kappa b ligand/osteoprotegerin. *Journal of endodontics* **2012**, *38*, 943-947.
21. Najeeb, S.; Zafar, M.S.; Khurshid, Z.; Zohaib, S.; Madathil, S.A.; Mali, M.; Almas, K. Efficacy of metformin in the management of periodontitis: A systematic review and meta-analysis. *Saudi Pharmaceutical Journal* **2018**, *26*, 634-642.
22. Jeyabalan, J.; Shah, M.; Viollet, B.; Chenu, C. Amp-activated protein kinase pathway and bone metabolism. *The Journal of endocrinology* **2012**, *212*, 277-290.
23. LeBrasseur, N.K.; Kelly, M.; Tsao, T.S.; Farmer, S.R.; Saha, A.K.; Ruderman, N.B.; Tomas, E. Thiazolidinediones can rapidly activate amp-activated protein kinase in mammalian tissues. *American journal of physiology. Endocrinology and metabolism* **2006**, *291*, E175-181.
24. Kanazawa, I.; Yamaguchi, T.; Yano, S.; Yamauchi, M.; Sugimoto, T. Metformin enhances the differentiation and mineralization of osteoblastic mc3t3-e1 cells via amp kinase activation as well as enos and bmp-2 expression. *Biochemical and biophysical research communications* **2008**, *375*, 414-419.
25. Lee, Y.-S.; Kim, Y.-S.; Lee, S.-Y.; Kim, G.-H.; Kim, B.-J.; Lee, S.-H.; Lee, K.-U.; Kim, G.-S.; Kim, S.-W.; Koh, J.-M. Amp kinase acts as a negative regulator of rankl in the differentiation of osteoclasts. *Bone* **2010**, *47*, 926-937.
26. Mizukami, J.; Takaesu, G.; Akatsuka, H.; Sakurai, H.; Ninomiya-Tsuji, J.; Matsumoto, K.; Sakurai, N. Receptor activator of nf-κb ligand (rankl) activates tak1 mitogen-activated protein kinase kinase kinase through a signaling complex containing rank, tab2, and traf6. *Molecular and Cellular Biology* **2002**, *22*, 992-1000.
27. Zhou, Z.; Han, J.-Y.; Xi, C.-X.; Xie, J.-X.; Feng, X.; Wang, C.-Y.; Mei, L.; Xiong, W.-C. Hmgb1 regulates rankl-induced osteoclastogenesis in a manner dependent on rage. *Journal of Bone and Mineral Research* **2008**, *23*, 1084-1096.
28. Palamoor, M.; Jablonski, M.M. Comparative study on diffusion and evaporation emulsion methods used to load hydrophilic drugs in poly (ortho ester) nanoparticle emulsions. *Powder Technology* **2014**, *253*, 53-62.
29. Martinez, N.Y.; Andrade, P.F.; Duran, N.; Cavalitto, S. Development of double emulsion nanoparticles for the encapsulation of bovine serum albumin. *Colloids and surfaces. B, Biointerfaces* **2017**, *158*, 190-196.
30. Iqbal, M.; Zafar, N.; Fessi, H.; Elaissari, A. Double emulsion solvent evaporation techniques used for drug encapsulation. *International journal of pharmaceutics* **2015**, *496*, 173-190.